Effect of Particle Shape on Hydrocyclone Classification

Kouki KASHIWAYA[a1], Takahiko NOUMACHI[a2], Naoki HIROYOSHI[a], Mayumi ITO[a], and Masami TSUNEKAWA[a]

[a] Graduate School of Engineering, Hokkaido University, Kita13, Nishi8, Kita-ku, Sapporo, Hokkaido, 060-8628, JAPAN

Corresponding author: Kouki Kashiwaya
Graduate School of Science and Technology,
Kumamoto University

Address
Kumamoto University Academic Commons Kurokami-3-611,
2-39-1 Kurokami, Kumamoto, 860-8555, JAPAN
TEL&FAX +81-96-342-3092
E-mail kasiwaya@kumamoto-u.ac.jp

Abstract

Influence of particle shape on hydrocyclone classification was investigated. Classification tests using hydrocyclone and cyclosizer showed that coarse fractions of plate-like particles such as PTFE and glass flake used here were not necessarily recovered as underflow product, especially at relatively high inlet velocity. Settling velocity of the glass flake particles in centrifugal field was estimated using a centrifugal particle size analyzer, and it was revealed that differences in settling velocity between coarse and fine glass flake particles became smaller with increases in angular velocity.

---

[1] Present address: Graduate School of Science and Technology, Kumamoto University, 2-39-1, Kurokami, Kumamoto, 860-8555, JAPAN

[2] Present address: Japan Petroleum Exploration Co., LTD., 85-2, Azahirune, Terauchi, Akita, 011-0901, JAPAN

Moreover, settling test of glass plate in water or glycerin solution was conducted to know relationship between particle Reynolds number (Re) and settling velocity of the plate. At smaller Re condition, the glass plate settled straight and stably, and larger plate settled faster than smaller plate. However, oscillating motion of the plate occurred in the region of high Re, and settling velocities of the large plate became smaller than that of the small plate in such conditions. Drag coefficient (C) calculated based on the settling velocity of the glass plate is similar to that of glass spheres below Re of about 50, above which it became larger than that of glass sphere. Approximation formula of correlaton between Re and C suggests that the influence of the Re on C can be neglected in the region of high Re, and C increases with increases in the ratio of the particle diameter to thickness (D/T).

The decrease of the difference in settling velocity recognized in the centrifugal settling test and the effect of the particle shape (D/T) on C at high Re region are considered to be able to affect the hydrocyclone classification. The misplacement of coarse plate-like particles in the hydrocyclone and cyclosizer tests could be ascribed to the particle shape effects.

Keywords: hydrocyclone, centrifugal field, gravitational field, classification, particle shape, drag coefficient

1. Introduction

The hydrocyclone is widely utilized for the purposes of classification, de-sliming, de-gritting, thickening, and so on, in the field of mineral engineering [1]. It has strong points such as simplicity in structure, smallness, and low cost relative to competitive equipments [2], and the application of hydrocyclones has recently extended to many other fields [3].

The flow condition inside hydrocyclones is complicated and thus models for separation with hydrocyclones are still not fully developed [4]. Especially the effect of particle shape on hydrocyclone separation is not sufficiently understood. There are numerous investigations of the settling velocity and drag coefficient of irregularly shaped or non-spherical particles in

gravitational fields [5-13]. However there are few reports describing the effect of particle shape on the settling and separation behavior in hydrocyclones, except a paper on the application of hydrocyclones to shape separation of fine particles [14]. It is known that plate-like particles such as mica are often discharged as overflow even though they are relatively coarse [1]. To control operation at optimum conditions and optimize separation efficiency, the effect of particle shape on the separation performance of hydrocyclones is in urgent need of further investigation.

This paper reports classification tests with hydrocyclones and cyclosizers (a particle size distribution analyzer with five hydrocyclones), carried out to compare the classification behavior of plate-like particles and spherical or block-shaped particles. The settling velocity of the particles in the centrifugal field was estimated with a centrifugal particle size distribution analyzer. Additionally, settling test of glass plates under gravitational field was carried out and drag coefficient of the plate-like particles is discussed related to the particle Reynolds number. Based on the experimental results, the classification properties of the particles in the hydrocyclone and cyclosizer are interpreted.

2. Materials and experimental methods

Polytetrafluoroethylene (PTFE) powder, glass flakes, and quartz powder were used as commercially available.

The PTFE powder (Hitachi Cable, Ltd.) was the same as that used in a previous investigation [15], and had a white powdery appearance with the maximum diameter of 88 μm and a mean particle size (d_{50}) of 21 μm, measured using a particle size analyzer (Microtrac MT3300SX, Microtrac Inc.), the density measured with a Ultrapycnometer 1000 (Quantachrome Instruments) was 2197 kg/m^3. Fig. 1a shows a microphotograph of the PFTE particles taken with a scanning electron microscope (SSX-550, Shimadzu Corporation), indicating that the PTFE particles have a plate-like shape with whiskers on the edges.

The glass flake (RCF-160, Nippon Sheet Glass Co., Ltd.) has a whitish clear appearance, and consists of plate-like particles of C-glass. The sample,

pulverized in a disc mill followed by sieving, was used in the classification tests. The maximum particle size of the pulverized glass flake sample was 249 μm and the d_{50} was 20 μm. The density was 2477 kg/m^3. The particle shape of the glass flakes is plate-like and similar to the PTFE particles (Fig. 1b), but not skewed and the edges are apparently sharper than the PTFE particles (Fig. 1a).

The quartz powder is pulverized and sieved quartz sand (Wako Pure Chemical Industries, Ltd.). The maximum particle size and d_{50} of the quartz sample were 105 μm and 11 μm, and the density was 2650 kg/m^3. The SEM micrograph shows that the quartz particles are block-shaped (Fig. 1c) and obviously different from the PTFE and glass flake samples.

These powders were mixed in dispersion media to make slurries and fed to the hydrocyclone tests. As the dispersion media distilled water was used for the glass flake and quartz powder, and for the PTFE powder surfactant solution containing Nonion NS-208.5 (NOF CORPORATION) was prepared. The PTFE surface is strongly hydrophobic, and a stable slurry cannot be prepared with only distilled water. The PTFE powder disperses in the surfactant solution equally well as in 2-propanol [15].

A schematic diagram of the hydrocyclone system used for the size clasification is shown in Fig. 2. The hydrocyclone equipped in the system is GMAX1U-3125 (FLSmidth Krebs Engineers) with diameter of 2.5 cm. The length of the hydrocyclone is 56 cm, and aperture diameters of the inlet, the voltex finder, and the apex are 1.91 cm, 0.70 cm, and 0.20 cm, respetively.

Principle of hydrocyclone classification can be summarized as below [1]. Slurry introduced into hydrocyclone makes vortex, and particles in the slurry are subjected to centrifugal (outward) force and drag (inward) force. It is known that behavior of particle in hydrocyclone can be estimated with Stoke's law, and as can be expected from this fact, the particles are classified based on their size and specific gravity. Downward flow and upward flow exist in outer region and inner region in hydrocyclone. Quickly settling particles by the greater centrifugal force move outward and are discharged with the downward flow from apex as underflow product. Slower settling particles by the greater drag force are discharged with the upward flow from

vortex-finder as overflow product.

The hydrocyclone tests were carried out as follows: 30 L of the slurry, prepared as described above, in the slurry tank was circulated by the circulation pump through the circulation line to agitate and disperse the particles in the slurry. After the slurry flow had stabilized, the valve on a feed line connected to the hydrocyclone was opened and the circulation line was shut off. After the slurry flow through the hydrocyclone reached a steady-state, the overflow product (hereafter referred to as OP) from the vortex finder and the underflow product (UP) from the apex of the cyclone were sampled in plastic bottles. In addition, the flow rates of the overflow and underflow were measured using measuring cylinders and a stopwatch. Both the overflow and underflow products were dried, and the solids were weighed for calculations of the solid concentrations of the OP and UP as the solid mass per unit volume of the samples.

Size distributions of particles contained in the OP and UP samples were measured using a laser-diffraction-dispersion-type particle size distribution analyzer, Microtrac MT3300SX (Microtrac Inc.), with the measurement condition: wavelength of light source, 780 nm; measured range of particle size, 0.021-1408 μm; measuring time, 30 s; refractive index, 1.55 for PTFE, 1.51 for glass flake, 1.33 for water; measure mode, transparent and nonspherical. Measurements for each sample were conducted twice and the average values calculated.

Recovery of particles with size d to UP ($R_{\mathrm{UP},\,d}$) is expressed by equation (2.1);

$$R_{\mathrm{UP},d} = \frac{c_{\mathrm{UP}} \times f_{\mathrm{UP},d} \times r_{\mathrm{UP}}}{c_{\mathrm{UP}} \times f_{\mathrm{UP},d} \times r_{\mathrm{UP}} + c_{\mathrm{OP}} \times f_{\mathrm{OP},d} \times r_{\mathrm{OP}}} \tag{2.1}$$

where, c_{UP} and c_{OP} are the solid concentrations of the UP and OP samples; $f_{\mathrm{UP},d}$ and $f_{\mathrm{OP},d}$ are frequencies of particles with size d in the particle size distribution of the UF or OF, and r_{UP} and r_{OP} are the flow rates of the underflow and overflow.

The cyclosizer, a particle size analyzer composed of five hydrocyclones, was modified and used as a classifier, and is shown in Fig. 3. The hydrocyclones are placed upside down and each hydrocyclone has a particle collector joined to the apex. The vortex finder of a hydrocyclone connects to the feed line of the next hydrocyclone. Large particles discharged from the apex of a hydrocyclone accumulates in the collector. The dispersive media runs into the collector, then returns to the hydrocyclone, agitating the trapped particles and giving opportunity for misplaced small particles to return to the hydrocyclone. Slurry containing smaller particles is discharged from the vortex finder and flows into the next hydrocyclone. The hydrocyclones are of the same size and shape, but the diameter of the feed lines become successively smaller from hydrocyclone No.1 to No.5 in a stepwise fashion. The inflow velocity of the feed to the hydrocyclone becomes faster moving to downstream hydrocyclones and thus increasingly smaller particle will be trapped in more downstream hydrocyclones. The outflow from the No.5 hydrocyclone is returned to the slurry tank, and the slurry circulates in the closed circuit. Particles trapped in the particle collector can be removed together with the dispersing media by opening the sampling valves. The hydrocyclones in the cyclosizer system can expel air cone through the sampling valves and the hydrocyclones are filled with slurry during the experiments. Because the PTFE powder is strongly hydrophobic, this cyclosizer is useful to investigate cyclone classification, ignoring the influence of any air-liquid interface on the classification. In the classification tests with the cyclosizer, 40 L of slurry was poured into the slurry tank and the circulation pump was turned on. Air cone in the hydrocyclone was expelled by opening the sampling valve for a while. After the experimental system reached a steady state (after 5 minutes), the slurry containing trapped particles was sampled from each hydrocyclone by operating the sampling valve. Particle size distributions of the products were measured with the particle size distribution analyzer used in the hydrocyclone test. Further, tests with glass spheres (diameter range: 10-40 μm; d_{50}: 30 μm; specific gravity: 2.5) were conducted for comparison, and 1.51 was employed as refractive index of the glass sphere in the particle size distribution

measurements.

A centrifugal type particle size analyzer (C-50, Shimadze Corp.) was used to investigate the influence of particle shape on settling velocity in centrifugal field. Schematic diagram of the equipment is shown in Fig. 4. Slurry containing sample particles was centrifuged in the transmissive disc cell of the C-50 analyzer at predetermined rotation speeds (500, 1000, and 1500 rpm). Settling velocities of the particles were interpreted based on the light intensity changes with time at a pre-determined point on the disc cell. In these experiments, the narrow sized fractions of quartz powders and glass flakes (-38 μm, +38-75 μm , and +75 μm) were used.

Further, gravitational settling tests of glass plates were conducted to study the relationship between particle Reynolds number and settling velocity, because the particles used in the other tests were fine, and did not allow direct observation of settling particles. The size of these glass plates were 5, 10, or 20 mm square, and 1 mm thick. The glass plates were placed individually, gently on the surface of 83 % glycerine or water in a cylinder (17.8 cm in diameter and 64.5 cm in height), and let sink in order to measure the settling velocity. The measurements were repeated 10 times under a predetermined condition and the reported settling velocity was the averaged value. The initial orientation of the glass plate placed on the solution before letting it sink was parallel or perpendicular to the solution surface. The experiments with glycerine were performed at different temperatures to adjust the solution viscosities, as shown in Table 1.

3. Results

3.1. Hydrocyclone test

Table 2 shows the experimental conditions of the hydrocyclone tests, with 8 runs for the PTFE, 5 runs for the quartz powder, and 11 runs for the glass flake.

Fig. 5 shows results of the hydrocyclone tests of the PTFE slurry, with the recovery of UP, the R_{UP} calculated using equation (2.1) was plotted against

inlet velocity. The recovery of fine particles (10-30 μm fractions) increased with increasing inlet velocity. However, the recoveries of medium-size particles (40 μm and 50 μm) showed a trend that is inconsistent with the finer particles, and the recoveries decreased repidly above 0.8 m/s of inlet velocity. Additionally, the recoveries of coarse particles (60 μm and 70 μm) varied in wide ranges.

For the quartz powder (Fig. 6), R_{UP} of finer particles (10-50 μm) almost consistently increased with increasing inlet velocity. The R_{UP} of coarser particles (60-80 μm) was constant, one, at any feed presure. These results correspond qualitatively to typical occurrences in hydrocyclone classifications, where increases in inlet velocity result in increases in the centrifugal force and consequently fine particles are recovered as underflow product.

Fig. 7 shows the results of hydrocyclone tests of the glass flake. R_{UP} of fine particles smaller than 50 μm increased with increasing inlet velocity. R_{UP} of midium-size particles (60-100 μm) also increased with inlet velocity even though some fluctuations were observed. For coarser particles (150-300 μm), R_{UP} fluctuated largely and the recovery of coarser particles was smaller than finer particles. The fluctuation on recovery of coarser particles was observed in the results of PTFE, too (Fig. 5).

3.2. Cyclosizer test

Table 3 shows the experimental conditions of the cyclosizer tests and pulp concentrations of PTFE and surfactant concentrations in the slurries. As shown in Fig. 3, cyclone No. 1 is located upstream and cyclone No. 5 is downstream. Coarser particles are generaly expected to be recovered in the upstream cyclones, depending on inlet velocity of the feed. Fig. 8 illustrates the size distributions of glass spheres recovered from the cyclones of the cyclosizer. For glass spheres, coarser particles were collected in the upstream hydrocyclone (Cyclone No. 1) and finer particles in downstream hydrocyclone (Cyclone No. 5). However, particle size distributions of the PTFE particles collected in the cyclones are obviously different from those of the glass spheres. They display several peaks and the frequency of the coarse particles

seems to be larger at the downstream hydrocyclone. Additionally, the maximum size of the collected particles is also larger at the downstream hydrocyclone.

3.3. Centrifugal settling test

Fig. 9 and Fig. 10 show the results of the centrifugal settling tests. The intensity of light transmitted through the disc cell and sample slurry increased with time, and finally reached constant value, indicating that the particles in the slurry settled by the centrifugal force. Fluctuations on the light intensity were observed soon after stating rotation. This can be attributed to change in depth of the slurry in the cell, and agitation of the slurry by starting rotation.

The time variation of the light intensity for slurries of the -38 μm fraction and the +38-75 μm fraction of quartz are similar (Fig. 9). The light intensity increased gradually and the rate of change became larger with increasing rotation speed. For the slurry of the +75-150 μm fraction, transmitted light intensity increased rapidly just after the beginning of rotation, and then increased gradually.

For the glass flake, the times to reach a steady-state intensity were the shortest at 1500 rpm or were similar at 1500 rpm and 1000 rpm, and longer at 500 rpm than 1500 rpm and 1000 rpm (Fig. 10). Additionally, more rapid increases in light intensity with time were observed for larger particles.

3.4. Gravitational settling test

Fig. 11 shows the relationship between viscosity of the solution and settling velocity of the glass plate.

When the glass plate was placed on the solution surface as the plate was parallel to the surface, the glass plate settled maintaining the original orientation in all experimental conditions. At higher viscosity, the plate setteled straight and stably. However, at lower viscosity, the settling behavior of larger plate (20 mm and 10 mm) became unstable and showed oscillating motion. The settling velocity of larger plate was larger at high viscosity, but, at low viscosity, the settling velocity of the larger plate became

smaller than smaller plate. This is because settling path became longer due to the oscillating motion at low viscosity condition.

When the plate was dropped as the plate was perpendicular to the solution surface, the plate rapidly changed its orientation parallel to the surface. After the rotation, the plate settled straight and stably at higher viscosity. At lower viscosity, the settling behavior, following the rotation soon after drop, became unstable and oscillating motion was observed. The larger plate settled faster at high viscosity, but settling velocity of larger plate became smaller than smaller plate by the oscillating motion at low viscosity. Additionally, 20 mm plate settled maintaining the initial perpendicular orientation at a viscosity of 0.001 Pa・s and its settling velocity was much larger than smaller plates.

4. Discussion

Particle size distribution obtained with the laser diffraction method is based on averaged projected area equivalent diameters [16], and it is known that particle shape strongly affects the result of particle sizing [17]. Additionally, it is also known that edge of particle produces high angle scattering and causes ghost peak of small particles in particle size distribution [18]. The particle size distributions in this paper were not adjusted relevant to the shape and edge effects. Considering the shape of PTFE, quartz, and glass flake, the particle size distributions may contain these effects. Therefore, the particle size distributions cannot be compared straightforwardly between PTFE, quartz, and glass flake, but particle size distributions are comparable in each sample, because they are expected to contain a similar degree of the sharp and edge effects. That is why the laser diffraction method was used for the particle sizing in this paper.

The results of the hydrocyclone tests showed that recovery of PTFE particles finer than 30 μm as underflow product became higher with increasing inlet velocity (Fig. 5). These results are simillar to the results for quartz (Fig. 6), indicating that increases in inlet velocity give rise to stronger centrifugal forces in the hydrocyclone and promote recover of fine particles as underflow products. For medium-size particles of PTFE (40μm and 50μm),

recovery decreased above 0.8 m/s inlet velocity. This may be caused by re-entrainment of the particles by increasing inlet velocity but similar phenomenon was not observed in the results of quartz. Additionally, fluctuation on recovery was observed in coarse particles (60μm and 70μm, Fig. 5). These results suggest that coarser PTFE particles were not necessarily recovered as underflow product, especially at higher inlet velocity.

Similar results were also obtained in hydrocyclone test of the glass flake (Fig. 7). Recovery of particles finer than 100 μm increased with increasing inlet velocity, but there is only a poor correspondence between the recovery and the inlet velocity for coarser particles (150-300 μm). The trend that recovery of coarser particle was smaller than finer particle was also recognized in the coarse particles. This means that coarser particles were more likely to be recovered as overflow product than finer particles. Considering that Fig. 5-7 were drawn based on the particle size distributions of the slurries collected at each inlet velocity condition, it could be said that this trend was presented repeatedly.

In the cyclosizer tests of glass spheres (Fig. 8), the size distribution of particles recovered by cyclones from No.1 (upstream) to No.5 (downstream) shifted to smaller sizes. But, with the PTFE particles the size distributions of the product recoverd by the cyclones located upstream (i.e. No.1 and No.2) had no coarser size region particles, suggesting that coarser particles are not recovered as underflow product, as also observed in the hydrocyclone test of PTFE and glass flake (Fig. 5 and Fig. 7).

These results indicate that classification behaviors of PTFE and glass flake are different from quartz and glass sphere, and the differences may be related to the particle shapes.

Centrifugal settling tests of the glass flake and quartz particles showed that the changes in transmitted light intensity with time and the rates of change were different for samples, size fractions, and angular velocities (rotation speed).

Particles in the slurry were assumed to be evenly distributed (after the agitation of the slurry by rotation), and the terminal settling velocity in the

centrifugal field is described by the following equation,

$$u = \frac{dr}{dt} = \frac{r\omega^2(\rho_p - \rho)}{18\mu} D_p^2 \quad (4.1)$$

where, u: terminal settling velocity, r: distance from axis of rotation, ω: angular velocity, ρ_p: particle density, ρ: density of dispersing media, μ: viscosity of the dispersing media, D_p: diameter of the particle.

The distance from the axis of rotation, density of the particles, density of the dispersing media, the viscosity of the dispersing media, and the diameter of the particle can be arbitrarily determined and thus considered as constant.

$$\frac{dr}{r} = \frac{\omega^2(\rho_p - \rho)}{18\mu} D_p^2 dt \quad (4.2)$$

When the distance between the rotation axis and the slurry surface is r_0, and the distance between the axis of rotation and measuring point for the transmitted light intensity is r_1 (Fig. 4), then integrating both sides from r_0 to r_1,

$$\ln \frac{r_1}{r_0} = \frac{\omega^2(\rho_p - \rho)}{18\mu} D_p^2 t \quad (4.3)$$

$$\omega^2 \propto \frac{1}{t} \quad (4.4)$$

Fig. 12 shows the relationships between ω^2 and 1/t in the centrifugal settling tests. The t values are the time necessary to reach 80 in transmitted light intensity in Fig. 9 and Fig. 10. In the Fig. 12, there are no obvious

differences in the slopes of the plots for the three size fractions of quartz. However the slopes for the glass flakes became flatter with increasing particle size, and almost reached zero for the 75-150 μm particles. The small slope in this figure means that the settling velocity of the coarser plate-like particles did not vary even though the angular velocity increased. In the hydrocyclones increases in inlet velocity correspond to increases in angular velocity. Therefore settling velocities of coarse plate-like particles and fine plate-like particles may become similar when inlet velocity increases in hydrocyclone.

Additionally, in the gravitational settling tests the settling velocity of smaller particles exceeded that of the larger particles at the lower viscosities of the dispersing media (Fig. 11), where larger plates oscillated and settling paths of particles became longer. Table 4 shows settling velocities and particle Reynolds numbers obtained in the gravitational settling tests. The results in the table suggest that the settling velocity of large particles is smaller than that of small particles when the particle Reynolds number is large.

When particles are settling at constant velocities in the gravitational field, the equation of motion for a particle is;

$$0 = \frac{m}{\rho_p}(\rho_p - \rho)g - CA\rho(\frac{u^2}{2}) \qquad (4.5)$$

Here, the drag coefficient (C) is

$$C = \frac{(\rho_p - \rho)Vg}{A\rho(\frac{u^2}{2})} \qquad (4.6)$$

and the particle Reynolds number (Re) is

$$\mathrm{Re} = \frac{D_p u \rho}{\mu} \qquad (4.7)$$

The drag coefficient and particle Reynolds number in the gravitational settling tests were calculated according to equations (4.6) and (4.7), and the results are shown in Fig. 13. The drag coefficient of the glass plates is similar to that of glass spheres below particle Reynolds numbers of about 50, above which it becomes larger than that of the glass spheres.

The drag coefficient varies depending on the inverse of the particle Reynolds number, thus the approximated drag coefficient was calculated as a function of the particle Reynolds number. The approximated drag coefficient C_a is expressed as

$$C_a = C_0 + C_1\left(\frac{1}{\mathrm{Re}}\right) \qquad (4.8)$$

and C_0 and C_1 were determined from the correlation of the particle Reynolds numbers and measured drag coefficients using the ratio of the particle diameter D to thickness T as the particle shape factor.

$$C_0 = 0.4555 \ln\left(\frac{D}{T}\right) + 0.4687 \qquad (4.9)$$

$$C_1 = 19.285 \qquad (4.10)$$

Finally, the approximated drag coefficient was expressed as

$$C_a = 19.285\left(\frac{1}{\mathrm{Re}}\right) + 0.4555 \ln\left(\frac{D}{T}\right) + 0.4687 \qquad (4.11)$$

This equation implies that the influence of the particle Reynolds number

on the drag coefficient can be neglected in the region of high particle Reynolds number, and the drag coefficient increases with increase in D/T. Here it must be noted that this relation was obtained from gravitational settling tests. Glass plates kept the orientation parpedicular to vertical except in one condition, and this settling behavior is consistent with results reported elsewhere [19, 20]. Different from the gravitational field, it is thought that the plate-like particles settle maintaining their orientations as their broad planes become parallel to the radial direction in a centrifugal field [21, 22]. However, flow conditions in simple centrifugal field and in hydrocyclone are significantly different because liquid rotates as a solid body in a centrifuge while the tangential velocity is inversely related to the radius in hydrocyclones [2]. As a result, the radial variation in the tangential velocity in hydrocyclones gives rise to a moment on plate-like particles and the particles may settle maintaining the orientations as their broad planes become perpendicular to the radial direction.

Kashiwaya et al. [15] interpreted the misplacement of particles based on a simple model of centrifugal, buoyancy, and drag forces, assuming that the particles settle as their broad planes become perpendicular to the radial direction in hydrocyclones. Centrifugal settling test in this paper revealed that difference in settling velocity between coarse and fine glass flake particles became smaller with increase in angular velocity. Further, the equation of approximated drag coefficient obtained in the gravitational settling tests indicated that the drag coefficient strongly depends on the ratio of the diameter to thickness of the particle. These particle shape effect can cause inefficient classification at high inlet velocity condition, and are considered to be related to the misplacement in the hydrocyclone test and cyclosizer test. To affirm the mechanism of the phenomenon explicitly, further detailed studies considering particle Reynolds numbers and the orientation of setlling particles in hydrocyclone separation are necessary.

5. Conclusions

Classification tests using hydrocyclones and a cyclosizer, centrifugal settling tests, and gravitational settling tests were conducted to investigate

the influence of particle shape on hydrocyclone classification.

In the hydrocyclone tests of PTFE and glass flake, recovery of coarser particles as underflow product decreased at high inlet velocities. Similar results were also obtained in cyclosizer tests and coarser PTFE particles recovered by the downstream hydrocyclones of the cyclosizer (at larger inlet velocities). The hydrocyclone and cyclosizer gave different results for quartz (block-shaped particles) and glass sphere (spherical particle), and the recovery of coarser particles increased with increasing inlet velocity in the hydrocyclone tests and coarser particles were collected by upstream cyclones (smaller feed velocity) in the cyclosizer tests.

The settling velocity in the centrifugal fields was estimated from centrifugal settling tests. The results show that the effect of the angular velocity was smaller for coarse particles of glass flakes than for quartz and finer particles of glass flakes. This means that differences in the settling velocity of coarse and fine particles in centrifugal fields become smaller with increasing angular velocity.

Additionally gravitational settling tests were carried out to observe the settling behavior of plate-like particles in liquids with different viscosities. In the region of higher particle Reynolds numbers, large particles oscillated and vertical settling velocities were smaller than those of smaller particles.

Approximated drag coefficient calculated based on the settling velocity of the glass plate depends on particle Reynolds number and the ratio of the particle diameter to thickness, but the influence of the particle Reynolds number on the approximated drag coefficient can be neglected in the region of high particle Reynolds number, and the drag coefficient increases with increase in the ratio of the particle diameter to thickness.

These particle shape effect can result in the misplacement in the hydrocyclone test and cyclosizer test, and are considered to be cause inefficient classification at high inlet velocity condition.

Acknowledgement

The authors gratefully acknowledge the financial and technical support provided by Hitachi Cable, Ltd. This research was conducted as a part of the

21st COE program of Hokkaido University.

References

[1] B.A. Wills, T. Napier-Munn, Wills' Mineral Processing Technology, seventh ed., Butterworth-Heinemann, Boston, 2006.
[2] E.G. Kelly, D.J. Spottiswood, Introduction to Mineral Processing, John Wiley & Sons, New York, 1982.
[3] L.-Y. Chu, W.-M. Chen, X.-Z. Lee, Enhancement of hydrocyclone performance by controlling the inside turbulence structure, Chemical Engineering Science. 57 (2002) 207-212.
[4] H. Schubert, Which demands should and can meet a separation model for hydrocyclone classification? Int. J. Miner. Process. 96 (2010) 14-26.
[5] J. Baba, P.D. Komar, Settling velocities of irregular grains at low Reynolds numbers. J. Sediment. Petrol. 51 (1981) 121-128.
[6] A.D.A. Chin, J. Portz, M. Ward, J.K. Beddow, A.F. Vetter, A shape-modified size correction for terminal settling velocity in the intermediate region, Powder Technol. 48 (1986) 59-65.
[7] F. Concha, A. Christiansen, Settling velocities of particulate systems, 5. Settling velocities of suspensions of particles of arbitrary shape, Int. J. Miner. Process. 18 (1986) 309-322.
[8] N.N. Clark, P. Gabriele, S. Shuker, R. Turton, Drag coefficient of irregular particles in Newton's settling regime, Powder Technol. 59 (1989) 69-72.
[9] A. Haider, O. Levenspiel, Drag coefficient and terminal velocity of spherical and nonspherical particles, Powder Technol. 58 (1989) 63-70.
[10] V. Ilic, J. Vincent, Sedimentation of complex-shaped particles in a square tank at low Reynolds numbers, Int. J. Multiphase Flow. 20 (1994) 445-452.
[11] M. Hartman, O. Trnka, K. Svoboda, Free settling of nonspherical particles, Industrial and Engineering Chemistry Research. 33 (1994) 1979-1983.
[12] Z.L. Arsenijevic, Z.B. Grbavcic, R.V. Garic-Grulovic, F.K. Zdanski, Determination of non-spherical particle terminal velocity using particulate

expansion data, Powder Technol. 103 (1999) 265-273.
[13] K.G. Tsakalakis, G.A. Stamboltzis, Prediction of the settling velocity of irregularly shaped particles, Minerals Eng. 14 (2001) 349-357.
[14] S. Endoh, H. Ohya, K. Masuda, S. Suzuki, H. Iwata, Study of the shape separation of fine particles using fluid fields –dynamic properties of irregular shaped particles in wet cyclones–, Kona. 12 (1994) 125-132.
[15] K. Kashiwaya, T. Noumachi, M. Ito, N. Hiroyoshi, M. Tsunekawa, Classification of fine hydrophobic particles using hydrocyclone, Proceedings of 9th Int. Symp. East Asian Recycling Technology. (2007) 661-664.
[16] K. Patchigolla, D. Wilkinson, M. Li, Measuring size distribution of organic crystals of different shapes using different technologies, Part. Part. Syst. Charact. 23 (2006) 138–144.
[17] M. Naito, O. Hayakawa, K. Nakahira, H. Mori, J. Tsubaki, Effect of particle shape on the particle size distribution measured with commercial equipment, Powder Technology. 100 (1998) 52-60.
[18] F. M. Etzler, R. Deanne, Particle size analysis: a comparison of various methods II, Part. Part. Syst. Charact. 14 (1997) 278-282.
[19] M. Göğüş, O.N. Ipekçi, M.A. Kökpinar, Effect of particle shape on fall velocity of angular particles, J. Hydraul. Eng. 127 (2001) 860-869.
[20] T. Tsuji, K. Yamaguchi, The relationships between particle shape and the terminal velocity in turbulent flow regions, Journal of the Society of Powder Technology, Japan. 24 (1987) 509-514.
[21] H. Brenner, The stokes hydrodynamic resistance of nonspherical particles, Chem. Eng. Commun. 148-50 (1996) 487-562.
[22] S. Torii, S. Tanaka, T. Yano, Y. Watanabe, Transport phenomena of circular disks suspended in centrifugal and non-centrifugal force environment, Functionally Graded Materials. 19 (2005) 13-18.

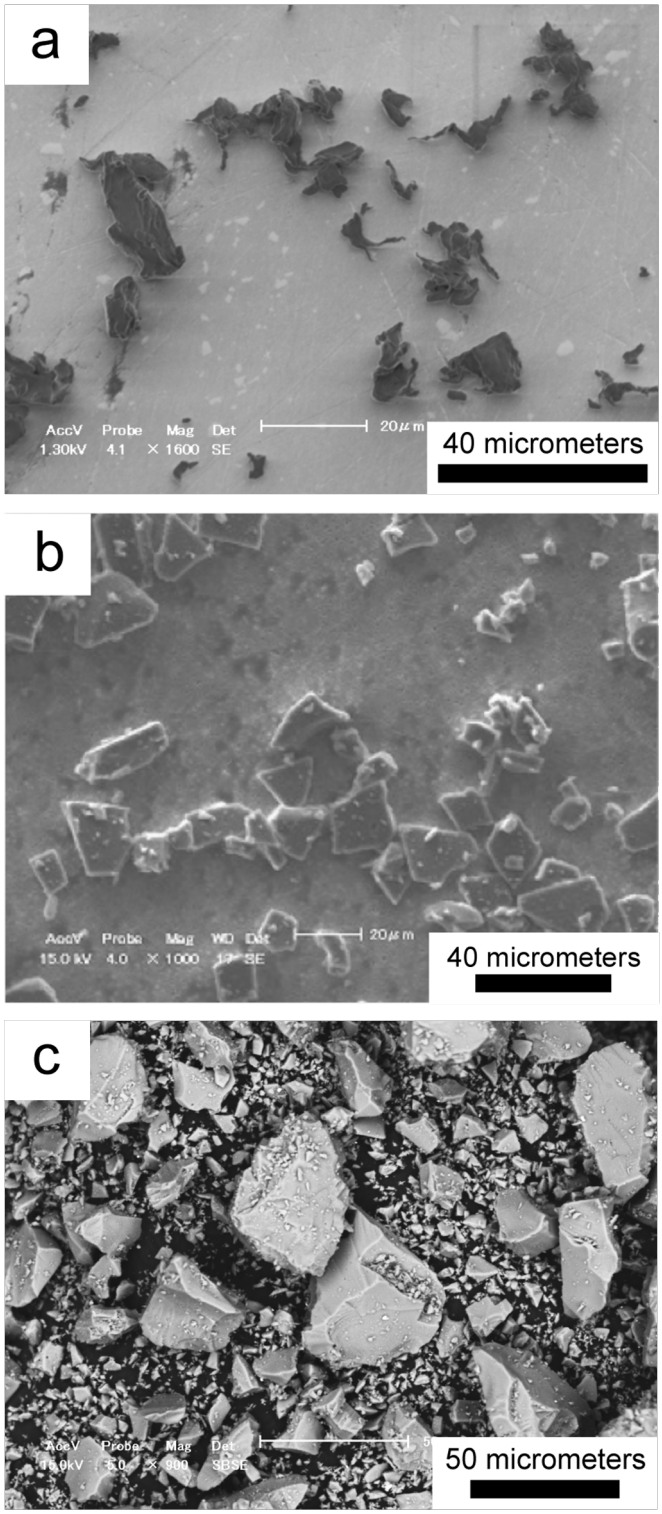

Fig. 1 Microphotographs of a) PTFE particles, b) glass flake particles, and c) quartz particles taken with scanning electron microscope.

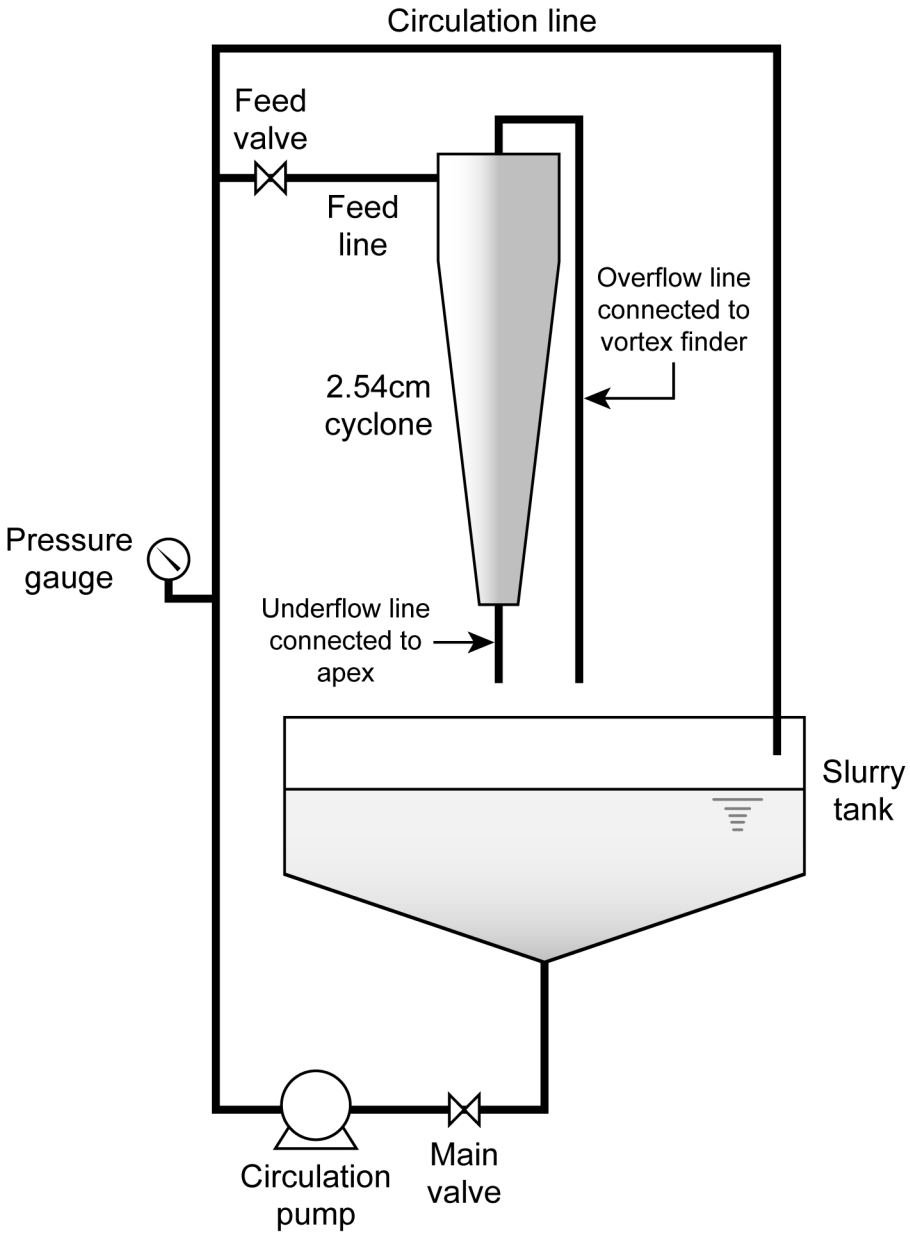

Fig. 2 Schematic diagram of the hydrocyclone arrangement.

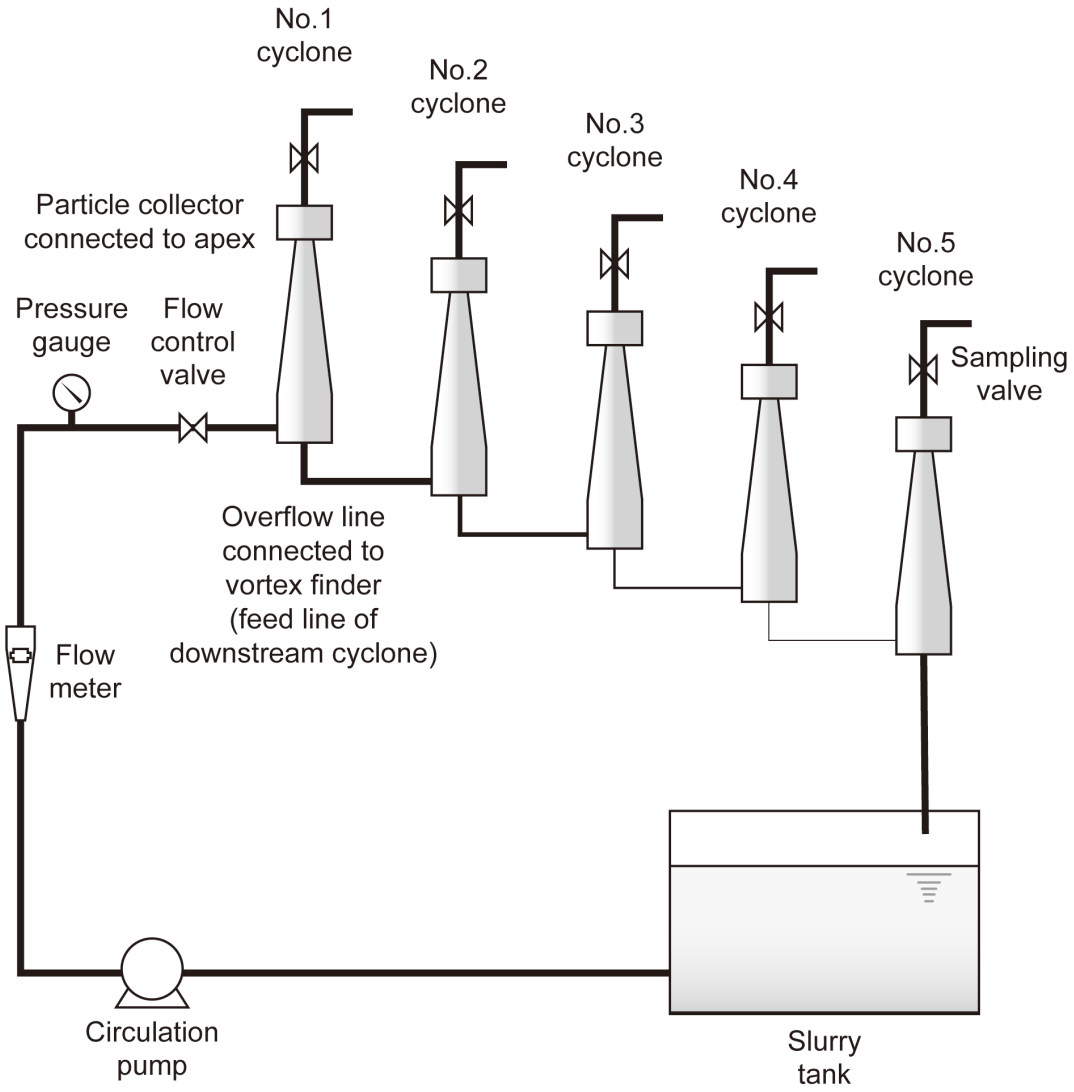

Fig. 3 Schematic diagram of the cyclosizer.

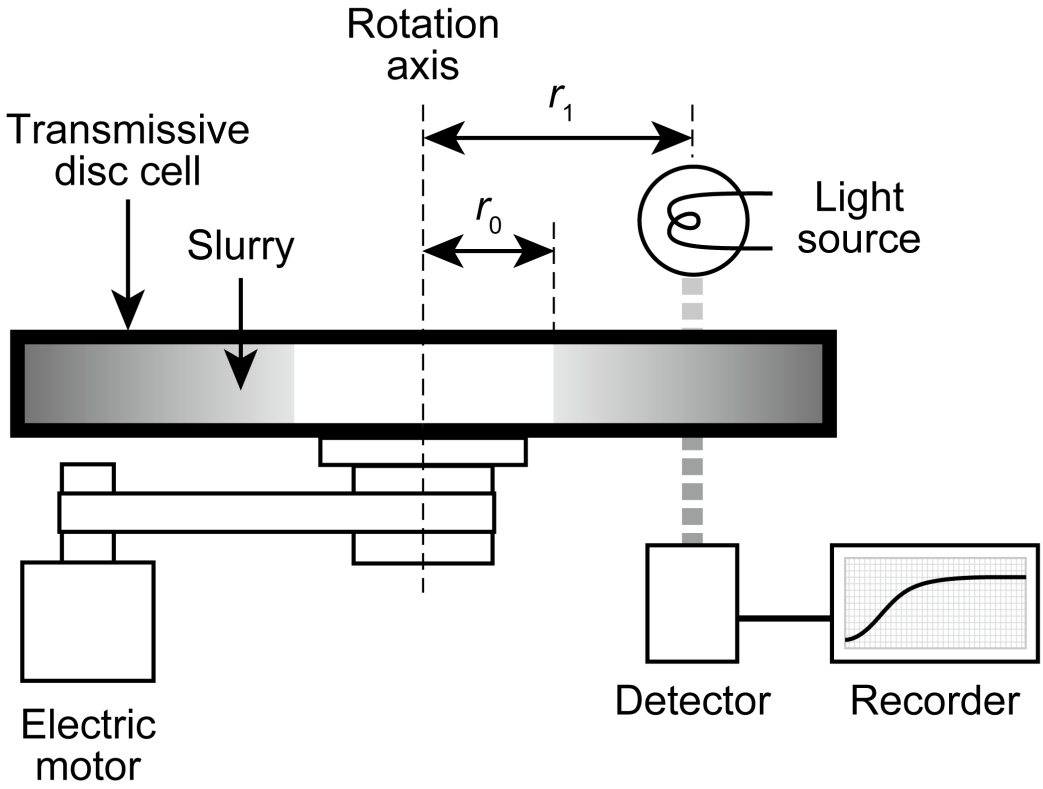

Fig. 4 Schematic diagram of the centrifugal type particle size analyzer.

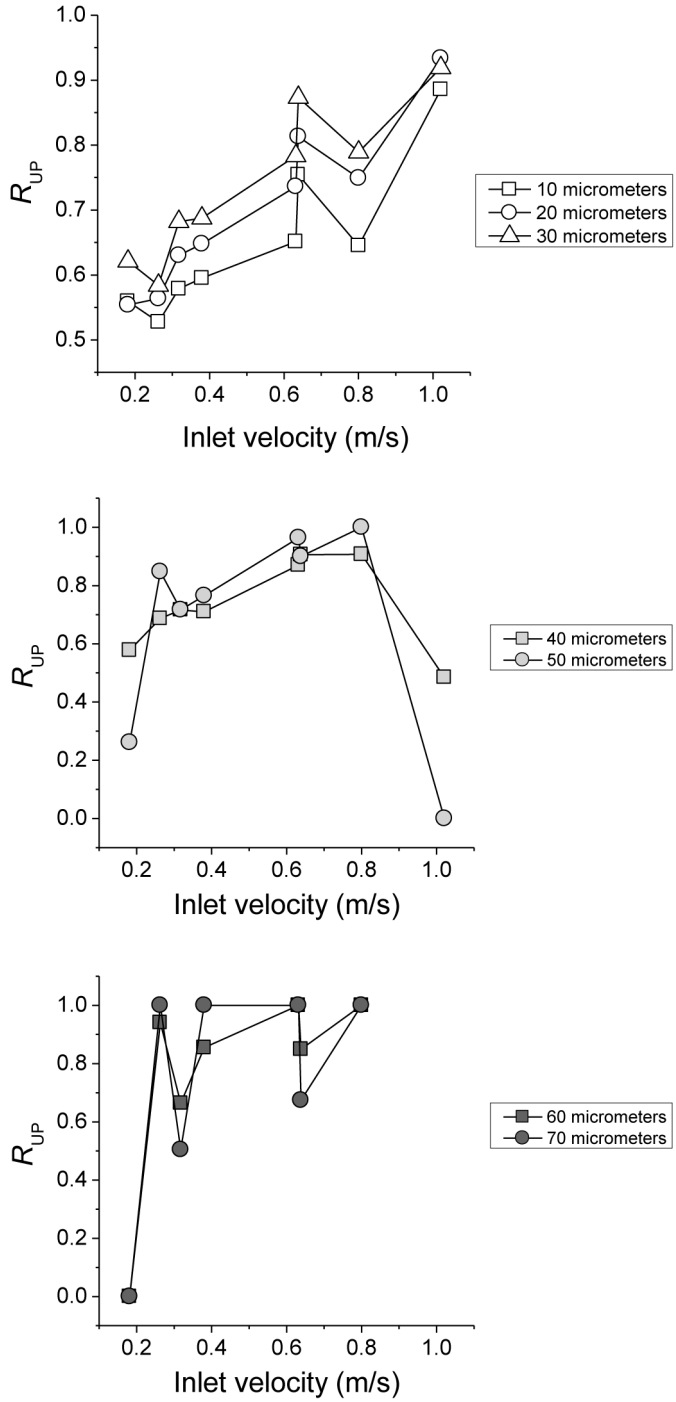

Fig. 5 Relationship between inlet velocity and recovery of underflow product for particles of different size fractions in the hydrocyclone classification of PTFE slurry.

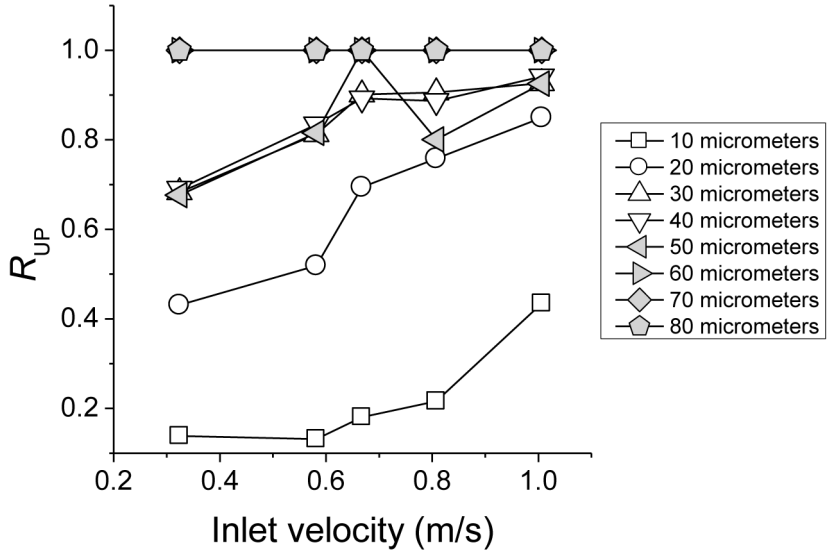

Fig. 6 Relationship between inlet velocity and recovery of underflow product for particles of different size fractions in the hydrocyclone classification of quartz slurry.

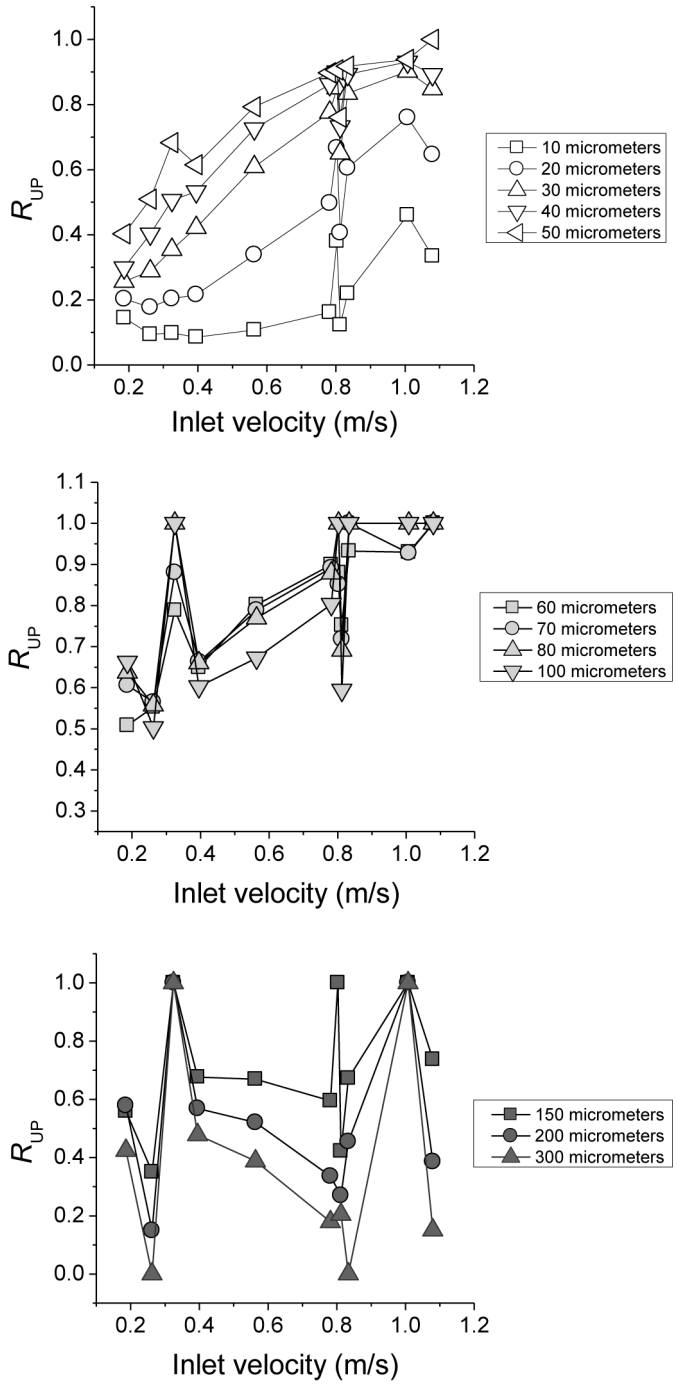

Fig. 7 Relationship between inlet velocity and recovery of different size fractions in the underflow product at the hydrocyclone classification of glass flake slurry.

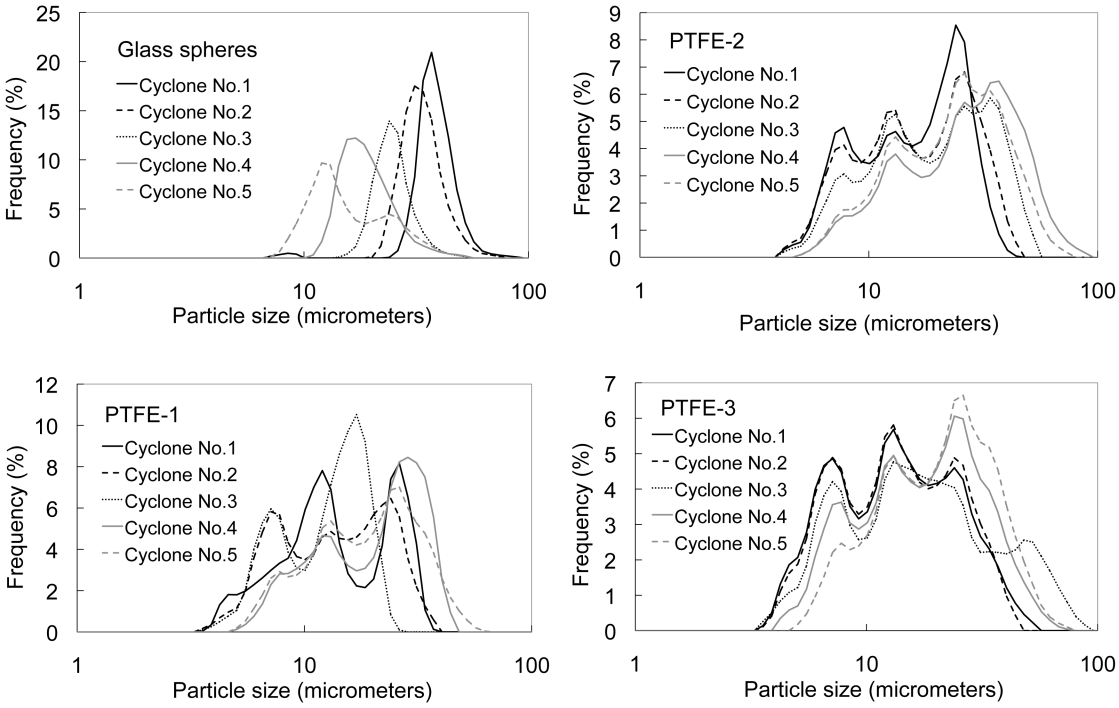

Fig. 8 Size distributions of fractions accumulated in each hydrocyclone in the cyclosizer.

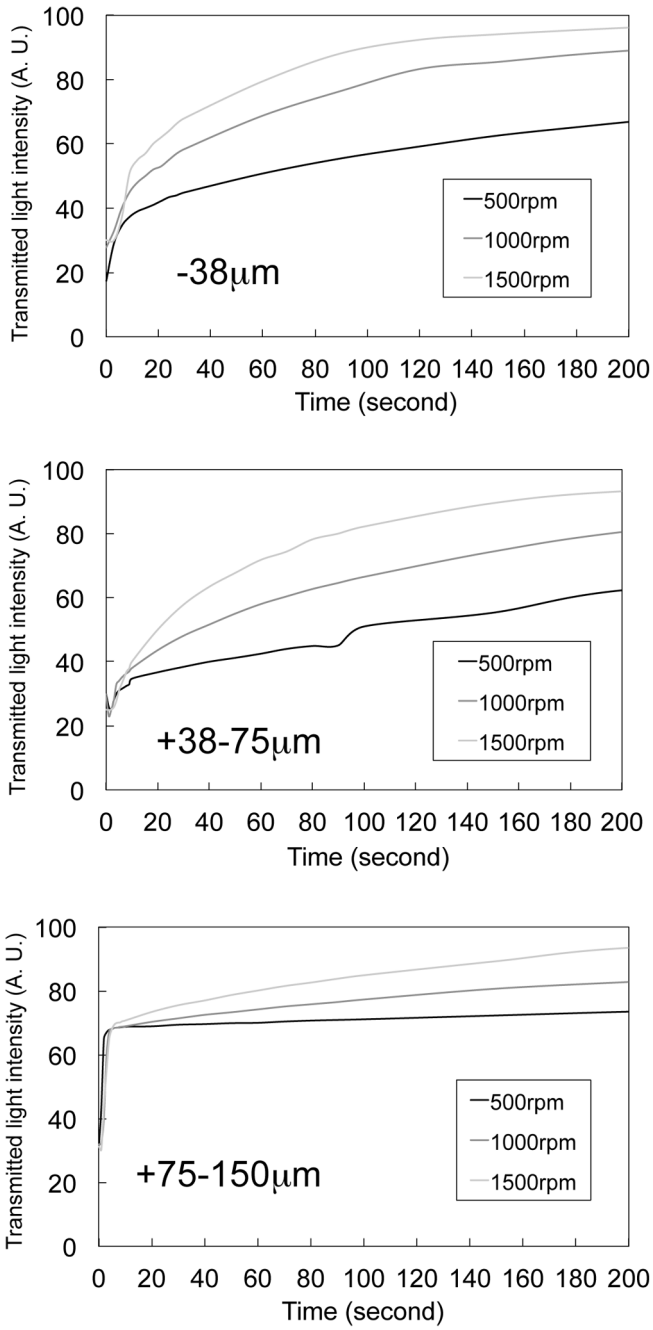

Fig. 9 Changes in light intensity transmitted through the quartz slurry and sample cell with time in the centrifugal settling tests.

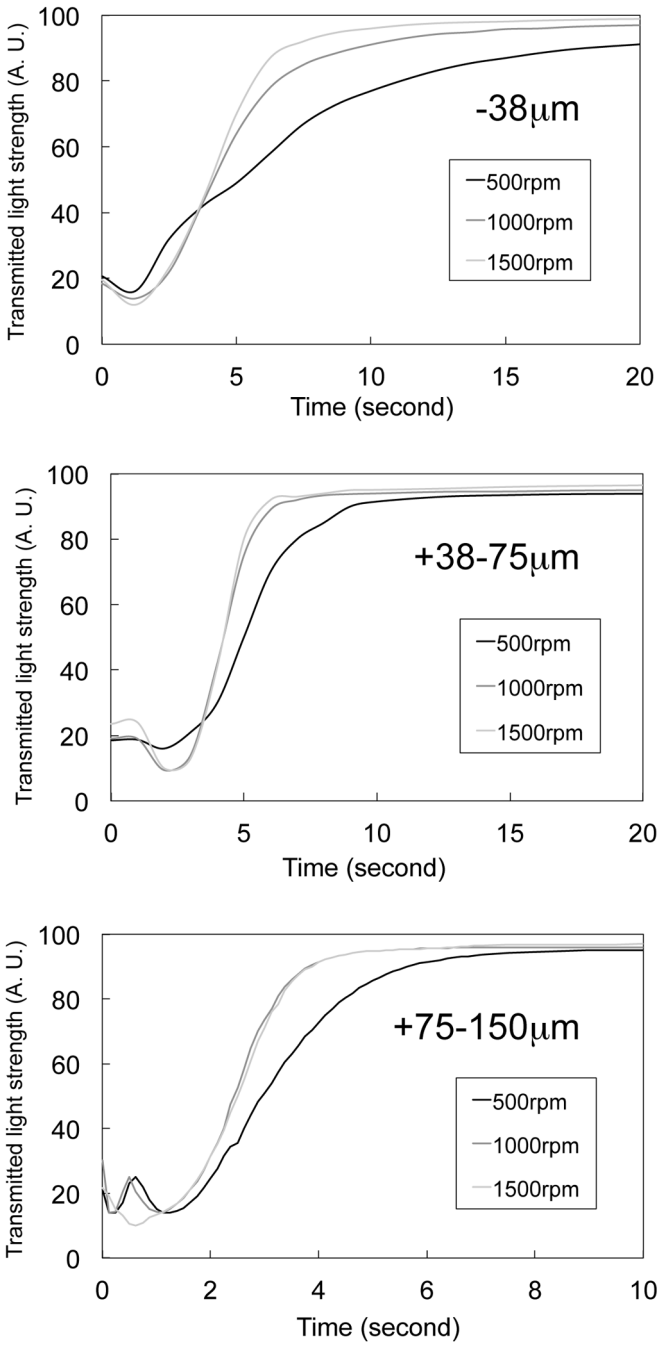

Fig. 10 Changes in light intensity transmitted through the PTFE slurry and sample cell with time in centrifugal settling tests.

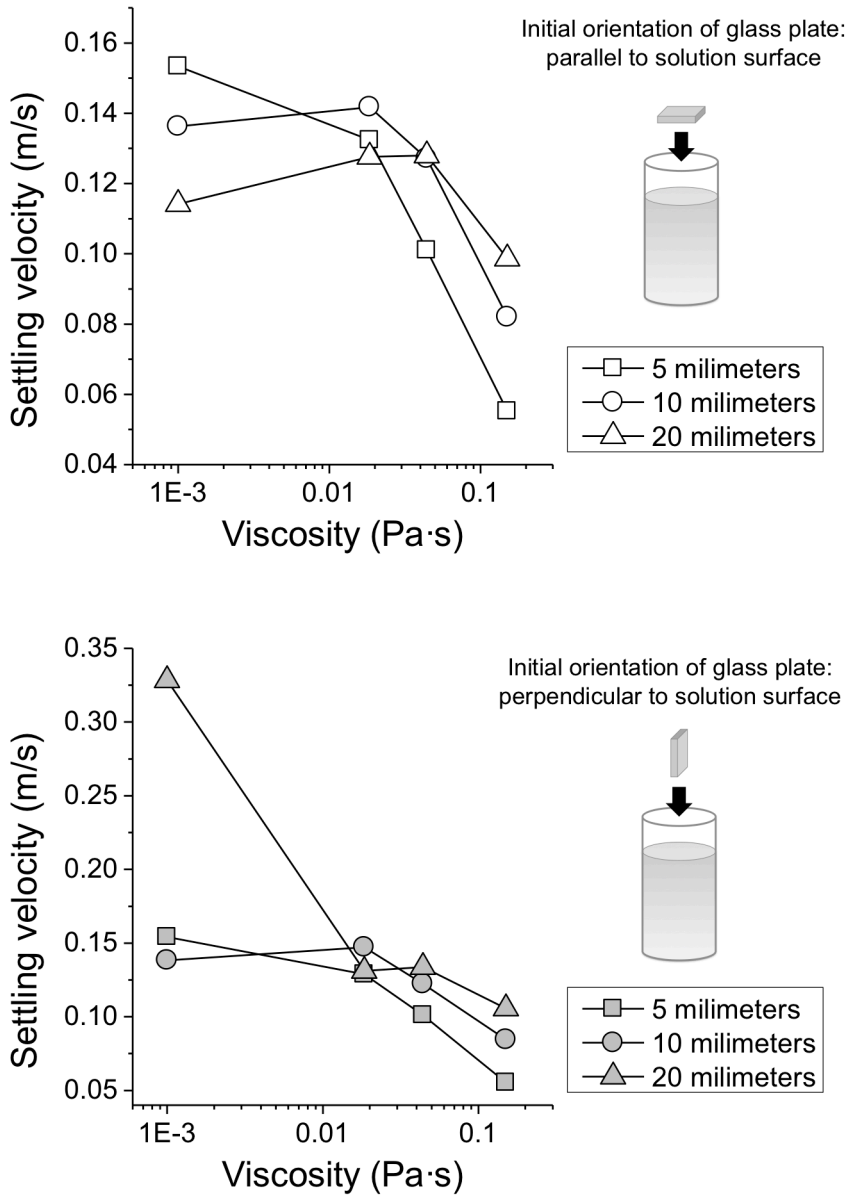

Fig. 11 Relationship between viscosity of liquid and settling velocity of the glass plates in the gravitational settling tests.

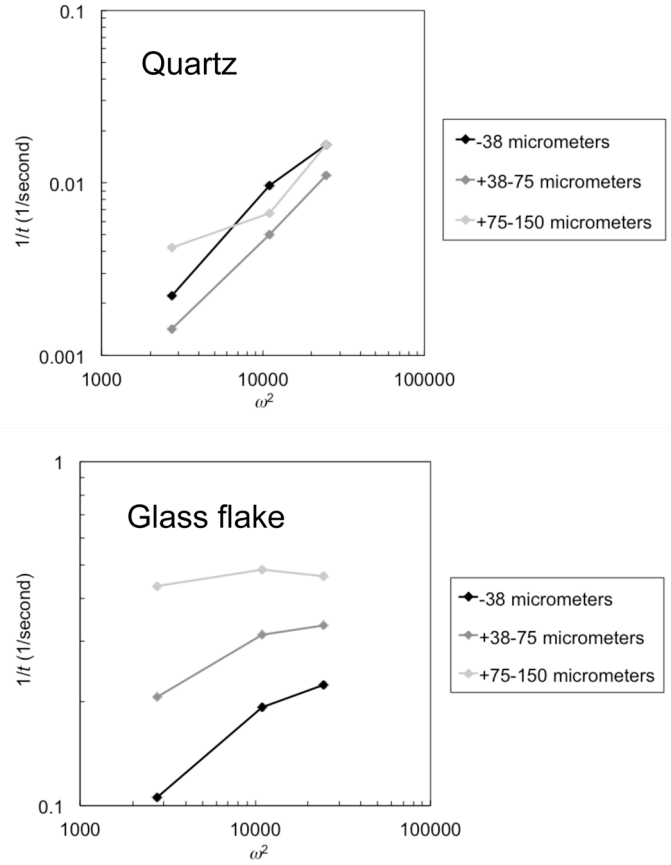

Fig. 12 Relationship between ω^2 and 1/t in centrifugal settling tests.

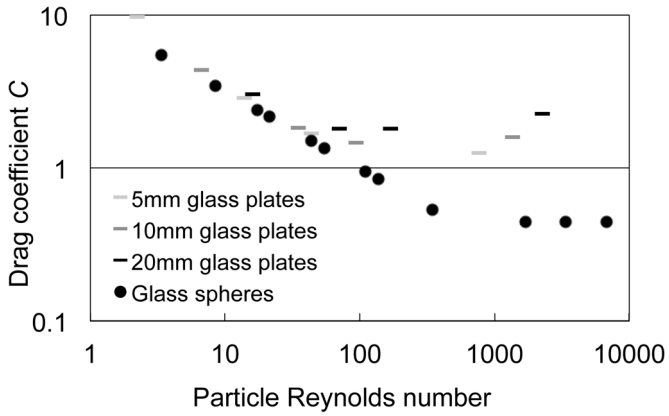

Fig. 13 Relationship between drag coefficient and particle Reynolds number in gravitational settling tests.

Table 1 Viscosities of the fluids used in the gravitational settling tests.

	83% glycerin	83% glycerin	83% glycerin	Water
Temperature	20°C	40°C	60°C	20°C
Viscosity (Pa・s)	0.15	0.044	0.0185	0.001

Table 2 Experimental conditions of the hydrocyclone tests.

No.	Sample	Solid concentration	Surfactant concentration	Feed pressure	Inlet velocity	Discharge rate of OF	Discharge rate of UF	Discharge ratio
		wt%	wt%	MPa	m/s	ml/s	ml/s	-
1	PTFE	0.1	0.002	1.0E-04	0.18	45.3	6.4	0.12
2				1.0E-02	0.26	68.6	6.5	0.09
3				2.0E-02	0.32	83.2	7.4	0.08
4				2.5E-02	0.38	100.3	8.0	0.07
5				5.0E-02	0.63	171.7	8.5	0.05
6				8.0E-02	0.64	167.4	14.6	0.08
7				1.0E-01	0.80	211.5	16.6	0.07
8				1.8E-01	1.02	260.4	30.6	0.11
9	Quartz	0.1	-	2.0E-02	0.32	81.5	10.8	0.12
10				5.0E-02	0.58	153.7	12.2	0.07
11				8.0E-02	0.67	175.3	15.1	0.08
12				1.0E-01	0.81	209.8	20.5	0.09
13				1.8E-01	1.01	242.7	44.2	0.15
14	Glass flake	0.1	-	1.0E-04	0.19	46.1	7.0	0.13
15				1.0E-02	0.26	67.2	7.6	0.10
16				2.0E-02	0.32	84.2	8.4	0.09
17				2.5E-02	0.40	103.4	9.2	0.08
18				5.0E-02	0.56	150.6	10.0	0.06
19				8.0E-02	0.81	218.3	13.3	0.06
20				1.0E-01	0.78	207.5	15.3	0.07
21				1.2E-01	0.83	219.7	17.8	0.08
22				1.4E-01	0.80	191.7	37.2	0.16
23				1.8E-01	1.08	264.7	42.9	0.14
24				2.0E-01	1.01	228.6	58.6	0.20

Table 3 Experimental conditions of the cyclosizer tests.

	Pulp concentration	Surfactant concentration	Flow rate	Pressure	Temperature
	wt%	wt%	L/min.	Mpa	°C
glass spheres	-	-	11.6	0.1927	22
PTFE-1	0.1	0.002	12.3	0.2202	23
PTFE-2	1	0.01	12.3	0.2202	23.4
PTFE-3			12.3	0.2202	26

Table 4 Settling velocity and particle Reynolds numbers in the gravitational settling tests.

Viscosity	Particle size	Settling velocity	Particle Reynolds number
Pa·s	mm	m/s	-
0.001	5	0.153	766.9
	10	0.136	1362.4
	20	0.114	2282.5
0.0185	5	0.132	43.6
	10	0.142	93.3
	20	0.128	167.9
0.044	5	0.101	14.0
	10	0.127	35.2
	20	0.128	70.8
0.15	5	0.055	2.2
	10	0.082	6.7
	20	0.099	16.0